Abstract

Geologists have long sought to understand the spatial distribution of erosion rates and their relationship to climate, topography, tectonics, and lithology. Since the mid-1980s, measurements of ^{10}Be, an *in situ* produced cosmogenic radionuclide, have been used to estimate bedrock outcrop and basin-scale erosion rates at >80 sites scattered non-uniformly around the world. Here, we compile and normalize published erosion rate data (n= 1531) in order to understand how, on a global scale, erosion rates vary between climate zones, tectonic settings, and different rock types. The large sample size allows us to test the relationship between erosion rates and a variety of landscape-scale parameters.

Drainage basins erode more quickly than bedrock outcrops. Outcrops (n=420) erode on average 16 ± 2.5 m My^{-1}; the distribution is highly skewed and the median rates is much slower, 5.2 m My^{-1}. On average, drainage basins (n=1111) erode more than 10 times faster than bedrock outcrops (209 ± 32.6 m My^{-1}); the median is much less, 53 m My^{-1}. In regions where both bedrock outcrop and basin-scale erosion rates have been measured, basins generally erode more quickly than outcrops, likely reflecting the acceleration of rock weathering rates under soil.

Bi-variate analyses indicates only weak correlation between erosion rates and landscape parameters on the global scale; correlations are much stronger at local scales. Landscape parameters best account for erosion rate variation when they are combined in multiple regression analyses. Such combinations explain, in the global data sets, 33% of the variability in bedrock erosion rates and 56% of the variability in basin-scale erosion rates. Basin-scale erosion rates are most often related to basin-average slope. Rock type is a major influence on bedrock outcrop erosion rates.

Introduction

Measuring the rate and spatial distribution of erosion on millennial timescales is fundamental to understanding how landscapes evolve through time and for placing human environmental impacts in context (Hooke, 1994, 2000). Yet, Geoscientists are largely lacking both the data and a global model to predict, with any accuracy or precision, the rate and spatial distribution of erosion on Earth's dynamic surface. We are even less able to predict how erosion rates respond to changes in boundary conditions including land use, tectonic, and climatic forcing. Clearly, rates of erosion are set by complex, non-linear feedbacks between multiple Earth systems including the solid Earth (tectonic uplift and rock shattering), the hydrosphere (rainfall intensity and distribution), and the biosphere (plants and soil biota); yet, these critical interactions occur on different temporal and spatial scales meaning that properties and relationships dominant at one scale may be unimportant at other scales.

Through the 20th century, geologists used a variety of tools to measure rates of erosion. The most common approach rates of erosion equated sediment yield with erosion rate. For example, compiling sparse data, Dole and Stabler (1909) made the first estimates of erosion rates for Northern America; later, Judson (1968) took a similar approach on a global scale. Such calculations presume that human impact on the landscape is inconsequential – refuted by Trimble (1977) – and that short-term measurements of sediment flux are representative of long-term flux rates – refuted by Kirchner et al. (2001).

Much of this early work was compiled by Saunders and Young (1983) who summarized erosion data from 420 publications. Erosion rates were estimated using a variety of methods in many different settings. The compilation shows that erosion rates differ by climate zone, that there was large variability between sites, and that erosion usually proceeds at less than 200 m My^{-1}. Rates varied by the active process and the scale of observation: rock weathering (1-130 m My^{-1}), chemical denudation (2-200 m My^{-1}), slope and cliff retreat (~100 m My^{-1}), and basin lowering (10-1000 m My^{-1}).

Until recently, no one method of measuring erosion rates directly was applicable world-wide. The development of Accelerator Mass Spectrometry (AMS) and the measurement of cosmogenic radionuclides, the concentration of which reflects near-surface residence time and thus the speed of many surface processes, has changed everything (Elmore and Phillips, 1987). Now, there is a globally applicable method for measuring erosion rates over millennial timescales. Geomorphologists have embraced these isotope systems enthusiastically. Since 1986, *in situ* produced cosmogenic radionuclides, most commonly ^{10}Be produced in quartz, have been used to model how quickly bedrock outcrops and river basins erode over geomorphically meaningful timescales (Bierman and Caffee, 2001; Bierman and Steig, 1996; Granger et al., 1996; Nishiizumi et al., 1986; Schaller et al., 2001; Small et al., 1997). Such modeling is based on the known behavior of cosmic rays that produce ^{10}Be, an otherwise exceptionally rare isotope, within the uppermost several meters of Earth's surface (Lal, 1991).

Many of the regional-scale cosmogenic studies, now numbering >80, indicate that physical and environmental parameters can influence millennial-scale erosion rates although the results are not uniform. In order to understand the relationship between erosion rates and metrics quantifying physical environmental parameters (e.g. climate, topography, biogeography, and tectonic setting) we compiled all publically available bedrock outcrop and basin-averaged erosion rates inferred from measurements of ^{10}Be. After normalizing the data for changes in calculation parameters used by different authors over the last 24 years, we compared erosion rates and a variety of physical parameters, both individually and using multivariate statistical methods. The result is a description, at a global scale, of the relationship between various environmental parameters and the erosion rate of both bedrock outcrops – and drainage basins. Such relationships can be used to predict erosion rates under different climatic and tectonic regimes and in areas where measurements have yet to be made and are thus important for understanding the behavior of Earth's sedimentary system over a variety of spatial and temporal scales.

Methods

We compiled all publicly available *in situ* ^{10}Be erosion rate data generated from fluvial sediment and bedrock outcrop samples (Figure 1; Tables 1, 2, & 3 in Data Repository). For outcropping bedrock, we included only unshielded samples collected from horizontal or sub-horizontal surfaces and in areas that had not experienced extensive recent glacial cover. For each sample, we collected all data necessary to recalculate erosion rates including reported ^{10}Be concentration, location coordinates, elevation, and the AMS standard (Table 1 in Data Repository). In some cases, information was provided in the original publications; in other cases, we contacted papers' authors directly.

Samples in this compilation required recalculation for two reasons: (1) constraints on production rates, neutron attenuation path length, and the ^{10}Be half-life have improved over time and values used in individual studies vary; (2) Some publications amend the erosion rate equation to correct for location-dependent anomalies such as geometric shielding, glacial history, and muon production, making it difficult to observe general global patterns from published erosion rates.

We used the CRONUS on-line calculator for erosion rate estimates (Balco et al., 2008): http://hess.ess.washington.edu/. Effective elevation, or the production-rate weighted average elevation for a basin, and effective latitude were determined from a MatLab script (see Data Repository), enabling us to use the CRONUS calculator for determining basin-wide erosion rates. CRONUS-calculated erosion rates for bedrock outcrops and basins strongly and significantly correlate to their original published erosion rates (see Data Repository).

We compared erosion rates for bedrock outcrop and basin samples to various environmental and physical parameters on the global-scale. For outcrop samples, these parameters include absolute latitude (°N or °S), elevation (m above sea level), relief (m within a 5 km radius), MAP (mm/yr), MAT (°C), and seismic hazard (a proxy for tectonic activity). For basin samples, we also consider average basin elevation (m above sea level), basin relief (m), basin area (km^2), mean basin slope (°), and percent vegetation cover (see Table 4 in the Data Repository)(Giardini et al., 1999; Hijmans et al., 2005; Peel et al., 2007). Data were extracted from global coverage datasets using ArcGIS software. Not all global coverages extend to Antarctica. Antarctic climate data was modified from Monaghan et al. (2006); seismicity data could not be gathered for Antarctica and so those sites are excluded from some of our analyses.

Analytical tests and statistics were run using JMP software. Bi-variate analyses were carried out for numeric parameters (i.e. MAP, MAT, seismicity, tree coverage, etc.) whereas analyses of variance and Student's t-tests were carried out for nominal data (i.e. climate zone, lithology, seismic regime). Forward stepwise regressions were carried out for each global dataset and for each subgroup of nominal data categories. Parameters were entered into the test based on their ability to statistically improve the regression; if a variable did not significantly improve the regression, it was omitted from the test. The parametric statistical tests we use assume a normal sample distribution. Because both bedrock and basin-scale erosion rate distributions are highly skewed (Figure 2), we log-transformed the erosion rate data before performing statistical tests.

Results

Bedrock outcrop erosion rates

Bedrock outcrops (n = 420) erode at an average rate of 15 ± 2.5 m My^{-1}. The median erosion rate is 5.2 m My^{-1}, indicating a skewed distribution (Figure 2a). Outcrop samples in the database are not uniformly distributed geographically and come from 4 clusters: the Antarctic, South America, southern regions of Africa and Australia, and mid-latitudes of North America and Europe (Figure 1). Most sample sites are between 30-40° latitude (Figure 3a). Sampling gaps between 50-70° reflect the absence of land in the Southern Ocean and the region of widespread glacial activity in the northern hemisphere; few samples have been collected from extremely low latitudes. Bedrock erosion rates are unrelated to absolute latitude, outcrop elevation, or seismicity (Figures 3a-c). Outcrops in seismically active regimes erode at 13 ± 1.6 m My^{-1} (n = 55), a rate indistinguishable from those in seismically inactive areas 16 ± 2.6 m My^{-1} (n = 367, Figure 3d). There is a weak, but significant correlation of outcrop erosion rates with relief (R^2 = 0.09; $p < 0.01$; Figure 3e). Outcrops are significantly related to MAP (R^2 = 0.15, $p < 0.01$, Figure 3f) and though no linear relation is observed with MAT, a peak in erosion rates centers around 10°C (Figure 3g).

An analysis of variance shows that outcrop erosion rates differ by lithology and that climate influences bedrock erosion rates. Sedimentary rocks erode at an average rate of 19 ±1.9 m My^{-1} (n = 106), which is significantly higher than the average erosion rate for metamorphic rocks (13 ± 1.7 m My^{-1}; n = 86; p = 0.03) and igneous rocks (8.6 ± 0.9 m My^{-1}; n =

232; $p < 0.01$, Figure 3h). The average outcrop erosion rate in temperate climates (35 ± 5.2 m My^{-1}; $n = 76$) is significantly higher than those in any other climate zone ($p < 0.01$; Figure 3i). Erosion rates for other climate zones also differ: cold (20 ± 4.0 m My^{-1}; $n = 111$), arid (7.7 ± 1.0 m My^{-1}; $n = 195$), tropical (7.2 ± 0.86 m My^{-1}; $n = 11$), and polar (3.8 ± 0.39 m My^{-1}; $n = 31$).

A forward stepwise regression shows that 33% of the variation of all bedrock outcrop erosion rates can be described by five significant parameters ($n = 424$; $R^2 = 0.33$; Figure 5a). Similar tests were run on bedrock outcrop erosion rates for individual climate zones, lithologies, and seismic regimes. Outcrop latitude, 5-km relief, and elevation are the most significant regressors. MAT moderately assists the regression of erosion rates in tropical climates and seismically inactive regimes.

Basin average erosion rates

On average, sampled drainage basins erode at 209 ± 33 m My^{-1} ($n = 1110$). The distribution is highly skewed with a median erosion rate of 53 m My^{-1} (Figure 2b). Basins selected for cosmogenic analyses are not randomly distributed; rather, sampling is biased toward mid-latitudes and temperate climates.

Landscape morphology is the strongest bi-variate control on drainage basin erosion rates. Basin slope yields the strongest correlation with erosion rates ($R^2 = 0.33$, $p < 0.01$; Figure 5a); basin relief and mean basin elevation also have significant positive correlations ($R^2 = 0.19$, $p < 0.01$; and $R^2 = 0.14$, $p < 0.01$, respectively; Figures 5b-c). Seismicity correlates to basin-scale erosion rates ($R^2 = 0.20$, $p < 0.01$; Figure 5d). The average erosion rate for basins in seismically active basins (365 ± 54 m My^{-1}, $n = 219$) is significantly higher than in seismically inactive basins (171 ± 27 m My^{-1}, $n = 810$, $p < 0.01$, Figure 5e). MAT has a very weak negative correlation ($R^2 = 0.08$, $p < 0.01$, Figure 5f) with drainage basin erosion rates. There is no significant correlation between basin erosion rates and latitude, MAP, or basin area (Figures 5g-i).

Basin-scale erosion rates differ by climate zone (Figure 5j). The average erosion rate in polar climates (554 ± 130 m My^{-1}; $n = 69$) is higher than in all other climate zones ($p < 0.01$): temperate (254 ± 35 m My^{-1}; $n = 465$), cold (158 ± 21 m My^{-1}; $n = 280$), tropical (116 ± 17.7 m My^{-1}; $n = 72$), and arid (102 ± 18 m My^{-1}; $n = 224$).

Typically, basins are underlain by one dominant lithology, though in some cases, the basins are so large, more than one type of lithology is prevalent. Basins in metamorphic terrains erode faster than any other lithology (288 ± 45 m My^{-1}; $n = 298$; $p < 0.08$, Figure 5k): mixed-lithology terrain (226 ± 37.5 m My^{-1}; $n = 292$), igneous (148 ± 19.6 m My^{-1}; $n = 302$) and sedimentary lithologies (163 ± 27.1 m My^{-1}; $n = 218$).

Forward stepwise regressions of basin erosion rates show that eight parameters describe 56% of variability ($R^2 = 0.56$; Figure 4b). Elevation was the only parameter not entered into the regression as its initial significance was too low to gain entry into the test. Nearly every basin-scale subcategories for which forward stepwise regressions were carried out indicate that basin slope is the most significant regressor; this includes the global regression. The remaining parameters are highly variable in terms of their regression power.

Discussion

Compilation of 1534 measurements of *in situ* produced ^{10}Be provides the first global view of erosion rates determined cosmogenically. The meta-analysis identifies five important themes: 1) Existing ^{10}Be data are non-uniformly distributed and have highly skewed distributions, 2) ^{10}Be erosion rates are consistent with those estimated by other techniques, 3) Basins erode more quickly than outcrops implying that regolith cover influences erosion rates, 4) Scale determines the degree of bi-variate correlation, 5) Environmental and material parameters allow better prediction of basin-scale than bedrock erosion rates.

1. Distribution of existing samples

Our compilation is global; however, large portions of Earth remain unsampled meaning that the data are non-uniformly distributed (Figure 1a). There are sampling gaps between 50-70° latitude, both north and south. Low latitude samples (0-10° north and south) are also rare. Latitudes with large sample populations, between 30-50° north and south, correspond to Europe, the United States, and Australia – easily accessible locations. Exceptions include large sample populations from basins and bedrock outcrops in Namibia and the Bolivian Andes (Bierman and Caffee, 2001; Cockburn et al., 2000; Kober et al., 2007; Kober et al., 2009; Safran et al., 2005; Wittmann et al., 2009). Refining the relationships presented in this study will happen only when these large spatial data gaps are filled.

Both bedrock and drainage basin erosion rates have highly skewed distributions (Figure 2) with most samples indicating relatively slow rates of erosion. This skewed distribution probably reflects the rapidity of erosion in tectonically active zones where mass is supplied to orogens by plate convergence and removed by rapid erosion of hillslopes at critical angles (Zeitler et al., 2001). In contrast, only isostatically driven rock uplift supplies mass for erosion in the tectonically stable zones that make up most of the world (Hack, 1975, 1979).

Studies with a large number of samples in one region (Bierman and Caffee, 2002; DiBiase et al., 2010; Henck et al., In Review; Safran et al., 2005; Schaller et al., 2001) are helpful in creating large sample populations for statistical analyses; however, sample adjacency leads to biases in data interpretation because of the scale dependance of correlation. For example, bedrock outcrops in cold climates come from numerous locations, geographically (n = 111) and the stepwise multivariate regression accounts for only 11% of the variability of erosion rates whereas 52% of variability of erosion rates in polar regions is explained. This high correlation is most likely the result of all 31 polar outcrop samples coming from a single, small geographic area.

2. Consistency of ^{10}Be erosion rates

Bedrock outcrop and basin-wide erosion rates determined cosmogenically are within the range of previously used techniques of quantifying erosion or denudation rates. Compiled bedrock outcrop erosion rates are slow (mean = 16 m My^{-1}; median = 5 m My^{-1}) and, with the exception of rare cases (Chappell et al., 2006), do not exceed 140 m My^{-1}, similar to rock weathering rates measured in the past which range from 2 – 200 m My^{-1} (Saunders and Young, 1983). Compiled basin-scale erosion rates (mean = 209 m My^{-1}; median = 5.2 m My^{-1}) also fall within previously published ranges as quantified by measuring chemical, bed, and suspended loads within rivers: 2-1000 m My^{-1} (Saunders and Young, 1983) and 4-690 m My^{-1} (Summerfield and Hulton, 1994), though in rare cases exceed these rates (Binnie et al., 2006; Binnie et al., 2008; Finnegan et al., 2007; Ouimet et al., 2009; Reinhardt et al., 2007; Vance et al., 2003; Wittmann et al., 2009; Wittmann et al., 2007); all of these extreme erosion rates are in seismically active regions (e.g. San Bernardino Mountains, Spanish Sierra Nevada) or in polar climates (e.g. Tibetan Plateau, Swiss Alps).

Drainage basin studies are ideally done in catchments where human impact is not obvious; however, as the human population increases, its role as a geomorphologic medium is more pronounced than ever (Hooke, 2000; Wilkinson and McElroy, 2007). As humans interact with larger areas of drainage basins, the natural sedimentation rates of drainages are altered and measuring the suspended load of a drainage basin no longer represents natural sedimentation or erosion rates (Kirchner et al., 2001; Syvitski and Milliman, 2007; Syvitski et al., 2005; Trimble, 1977).

3. Basins erode more rapidly than bedrock outcrops

Taken at face value, average bedrock outcrop erosion rates are more than ten times slower (16 m My^{-1}) than those inferred from basin-scale studies (209 m My^{-1}). Comparison of median values (5.2 versus 53 m My^{-1}) shows a similar relationship. Within each seismic regime, climate zone, and lithology, drainage basins are eroding more rapidly than bedrock outcrops. While it is possible that the location of bedrock versus basin-scale samples accounts for this bias, we consider such sampling bias unlikely because there are 19 regions around the world where both bedrock outcrop and basin erosion rates have both been measured (Figure 6). At all but 5 of those sites, drainage basins erode faster than bedrock outcrops. The five sites where bedrock outcrops erode faster than drainage basins are situated in stable regions such as passive continental margins (e.g. Shenandoah National Park, Blue Ridge Escarpment, and Great Smoky Mountain National Park in the United States) and inner-continental cratonic rocks (Flinders Range, Australia). However, not all sites along passive continental margins follow this pattern: for example, studies done in the Susquehanna River Basin (Reuter et al., 2006) and the Sri Lankan escarpment (von Blanckenburg et al., 2004) indicate that drainage basins are eroding more rapidly than bedrock. Large discrepancies between sample sizes for each of these regions produce average erosion rates which may not be representative of the region.

4. Influence of scale on erosion rates

Scale appears to determine which parameters influence both bedrock outcrop and drainage basin erosion rates because correlations observed on the local scale are often not observed or are much weaker on the global scale. For example, in Australia, the lowest measured bedrock outcrop erosion rate from sampling sites on Australia's Eyre Peninsula and in central Australia correlate well with MAP ($R^2 = 0.98$) (Bierman and Caffee, 2002). On the global scale, however, there is little correlation; MAP does not factor into the multivariate analysis for bedrock outcrop erosion in arid regions. On a basin-scale, erosion rates have been shown to correlate well with average basin elevation in individual studies (Heimsath et al., 2006; Palumbo et al., 2009). This relationship is only weakly seen at the global scale with mean basin elevations ($R^2 = 0.14$) and elevation is neither a dominant regressor in any of the multivariate regressions (Figure 5c). We suspect the scale-dependance of bivariate correlation is caused by the variety of other factors affecting erosion rates such as bedrock structure and strength.

Mean basin slope is the one parameter that influences basin-scale erosion rates significantly at both the local and global level. For example, mean basin slope produced the strongest bi-variate correlation with drainage basin erosion rates at the global scale ($R^2 = 0.33$, Figure 5a). At local scales, the correlation can be even better and many drainage basin erosion rate studies show a positive relationship between erosion rate and slope (Matmon et al., 2003; Palumbo et al., 2009; Reuter et al., 2006; Sullivan et al., accepted; von Blanckenburg et al., 2004). In the multivariate analyses, slope was the predominant regressor in nearly every subdivision of categorical data (Figure 4b), and was the predominant regressor for the global basin-scale multivariate regression.

5. Influence of material and environmental parameters on erosion rates

Lithology strongly influences the rate of bedrock erosion. Outcrops of sedimentary rock erode faster than both igneous and metamorphic outcrops, a difference that may be due to inherent weaknesses between sedimentary units, along bedding planes, and between individual grains. Crystalline rocks are naturally stronger as they are comprised of interlocking crystal grains; however, metamorphic rocks erode more quickly than igneous rocks, perhaps due to weaknesses along foliations. The influence of lithology on a basin scale erosion rates is different. Basins underlain by metamorphic rocks are eroding more quickly than basins underlain by igneous or sedimentary rocks. Most likely the control here is at least partially tectonic; metamorphic rocks often crop out in tectonically active zones.

Many studies (REF) indicate a coupled relationship between relief or slope and precipitation, indicating higher erosion rates in mountainous or steep terrain controlled by orographic processes, but these relationships are not apparent on a global scale (Figure 7).

Drainge basin erosion rates are clearly related to topographic metrics (relief and slope). On the global scale, relief and slope both produced a strong bivariate correlation with drainage basin erosion rates and is significant in numerous multivariate analyses including regressions for cold, tropical, and temperate climates, basins of mixed lithology, and seismically active regimes. On the local scale, relief and erosion rate co-vary in basins of the Tibetan Plateau (Finnegan et al., 2007; Palumbo et al., 2009) but other studies find no correlation of erosion rates with basin relief, such as in the Great Smoky Mountains of Tennessee and North Carolina (Matmon et al., 2003) and the Western French Alps (Delunel et al., 2010). Slope is related to erosion rates in most, but not all drainage basin studies (Riebe et al., 2001).

Other environmental parameters exert at most a weak control on outcrop and drainage basin erosion rates. MAP is frequently cited as a parameter controlling erosion rates and a relationship is often observed in local and regional studies of both bedrock and drainage basins (Bierman and Caffee, 2002; Bierman and Caffee, 2001; Henck et al., In Review; von Blanckenburg et al., 2004). However strong a correlation MAP produces at the local scale, globally only weak correlations are observed and multivariate analyses suggest MAP does not play an important role in explaining erosion rates for either outcrops or basins.

Globally, other individual landscape and climatic parameters yield only weak bivariate correlations with both outcrop and drainage basin erosion rates, but when combined, their ability to account for variability in erosion rate increases for individual groups of categorical data. For example, in cold climates, relief, slope, percent tree cover, basin area, MAP, seismicity, and latitude significantly account for 75% of variability in basin erosion rates. Among sedimentary rocks, seismicity, relief, mean annual precipitation, mean annual temperature, and elevation significantly account for 48% of variability in bedrock outcrop erosion rates (Figure 4a).

Implications for landscape evolution

The ten-fold offset between rates of bedrock outcrop erosion and those of drainage basins suggests that ridgelines, where bedrock outcrops are common, erode less rapidly than the surrounding basins. The offset between outcrop and basin-scale rates of erosion implies that relief is increasing in many study areas as ridges are lowered less rapidly than basins. Of course, this offset cannot continue forever. Ridgelines will eventually be consumed from their margins.

Bedrock and basin scale erosion rates are controlled by different processes and occur in different physical, chemical, and hydrological environments. Bedrock outcrops are situated above the landscape and exposed to a limited suite of largely ineffective sub-aerial erosion processes that both physically and chemically wear away exposed rock. The stability of bedrock outcrops is likely due to the xeric microclimate they create as precipitation rapidly runs off exposed rock surfaces. The conversion of bedrock to regolith through several linked chemical and physical processes include hydrolysis, weathering induced by organic acids, and the ability of soil to hold water over longer periods between precipitation events. A thin mantle of soil appears to create conditions most favorable for the conversion of bedrock to soil – the "humped" soil production function (Heimsath et al., 1997b, 1999).

Cosmogenic data show that spatial gradients of climate influence millennial-scale erosion rates. Thus, substituting time for space, glacial-interglacial climate cycles probably changed erosion rates and thus the flux of sediment shed off the landscape. Erosion rates are generally highest for both bedrock outcrops and basins in temperate and cold climate zones, peaking where the MAT is ~ 10°C (Figures 3g and 5f). Temperatures in these zones fluctuate throughout the year with numerous freeze-thaw cycles that may facilitate frost cracking on outcrops and cryoturbation on basin hillslopes (Delunel et al., 2010; Hales and Roering, 2007). This hypothesis is testable. Paleo-erosion rates should be higher than modern rates in areas where warmer climates cooled significantly during the Pleistocene.

Future Prospects

Compiling more than 20 years of cosmogenic analyses clearly shows their value in measuring background rates of erosion around the world and thus predicting long-term sediment generation rates at a variety of spatial scales; yet, the same compilation demonstrates spatial biases in the existing data set, providing both justification and guidance for filling in substantial data gaps. Most ^{10}Be measurements have been done in quartz-rich rocks and sediment because quartz retains *in situ* ^{10}Be, has a simple composition so nuclide production rates are easily calculated, and because it is a ubiquitous. However, ^{10}Be can be extracted from other minerals allowing ^{10}Be studies to be carried out in a variety of lithologies (Ivy-Ochs et al., 2007; Nishiizumi et al., 1990) and thus expanding the geographical area where erosion rates could be measured. Application of other isotope systems (such as ^{21}Ne, ^{3}He and ^{36}Cl) offer the potential to constrain better the effect of lithology on erosion rates (Kober et al., 2009); however, uncertainties in cross-calibration of production rates between different isotope systems would introduce biases into the data analysis.

Accurate, global prediction of background erosion rates is critical because erosion is the means by which sediment is generated, fresh rock is exposed to CO_2-consuming weathering reactions, soil is created, landforms change over time, and mass is moved from the continents to the oceans and eventually recycled *via* the process of subduction and volcanism. Earth's ability to support billions of inhabitants depends critically on the resiliency of the soil system and the purity of surface waters, both of which erosion affects directly. The compilation presented here indicates that such predictive capabilities are within our reach.

Figures

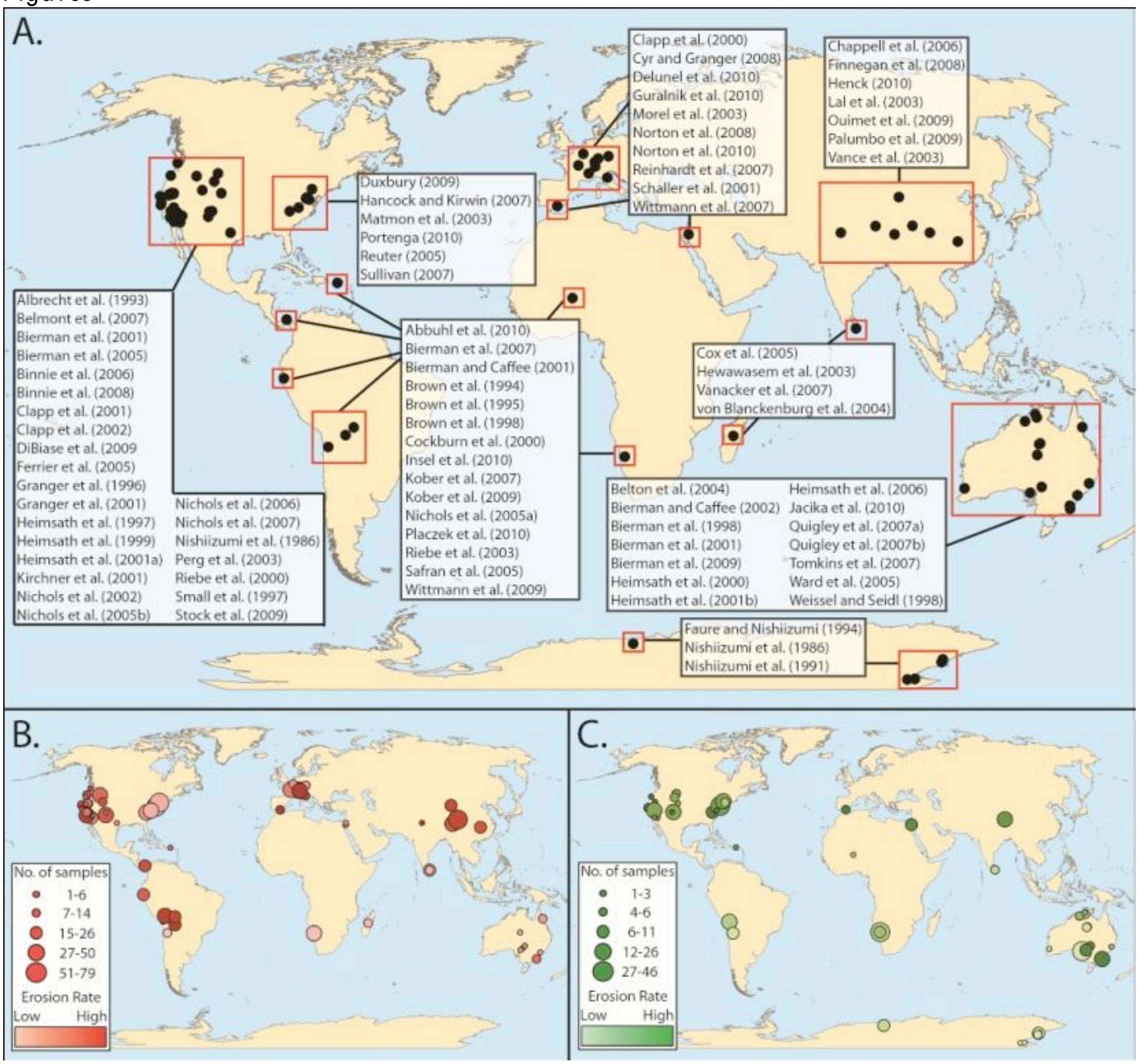

Figure 1. Global distribution of locations (A) of drainage basin (B) and bedrock outcrop (C) erosion rates have been derived using measurements of ^{10}Be (Abbühl et al., 2010; Albrecht et al., 1993; Belmont et al., 2007; Bierman et al., 1998; Bierman and Caffee, 2001; Bierman et al., 2001; Bierman et al., 2007; Bierman et al., 2005; Binnie et al., 2006; Binnie et al., 2008; Brown et al., 1994; Brown et al., 1998; Brown et al., 1995; Clapp et al., 2002; Clapp et al., 2001; Clapp et al., 2000; Cockburn et al., 2000; DiBiase et al., 2010; Duxbury et al., accepted; Ferrier et al., 2005; Granger et al., 1996; Granger et al., 2001; Hancock and Kirwan, 2007; Heimsath et al., 2006; Heimsath et al., 2000, 2001a; Heimsath et al., 1997a, 1999, 2001b; Insel et al., 2010;

Kirchner et al., 2001; Kober et al., 2007; Kober et al., 2009; Matmon et al., 2003; Nichols et al., 2005a; Nichols et al., 2007; Nichols et al., 2005b; Nichols et al., 2006; Nichols et al., 2002; Nishiizumi et al., 1986; Perg et al., 2003; Placzek et al., 2010; Portenga et al., 2010; Reuter et al., 2003; Riebe et al., 2003; Riebe et al., 2000; Small et al., 1997; Stock et al., 2009; Sullivan et al., accepted)(Belton et al., 2004; Bierman and Caffee, 2002; Bierman et al., 2009; Chappell et al., 2006; Cox et al., 2006; Cyr and granger, 2008; Delunel et al., 2010; Faure and Nishiizumi, 1994; Finnegan et al., 2007; Guralnik et al., 2010; Heimsath et al., 2006; Heimsath et al., 2000, 2001a; Henck et al., In Review; Hewawasam et al., 2003; Jakica et al., 2010; Lal et al., 2003; Morel et al., 2003; Norton et al., 2010; Norton et al., 2008; Ouimet et al., 2009; Palumbo et al., 2009; Quigley et al., 2007a; Quigley et al., 2007b; Reinhardt et al., 2007; Safran et al., 2005; Schaller et al., 2001; Tomkins et al., 2007; Vanacker et al., 2007; Vance et al., 2003; von Blanckenburg et al., 2004; Ward et al., 2005; Weissel and Seidl, 1998; Wittmann et al., 2009; Wittmann et al., 2007)

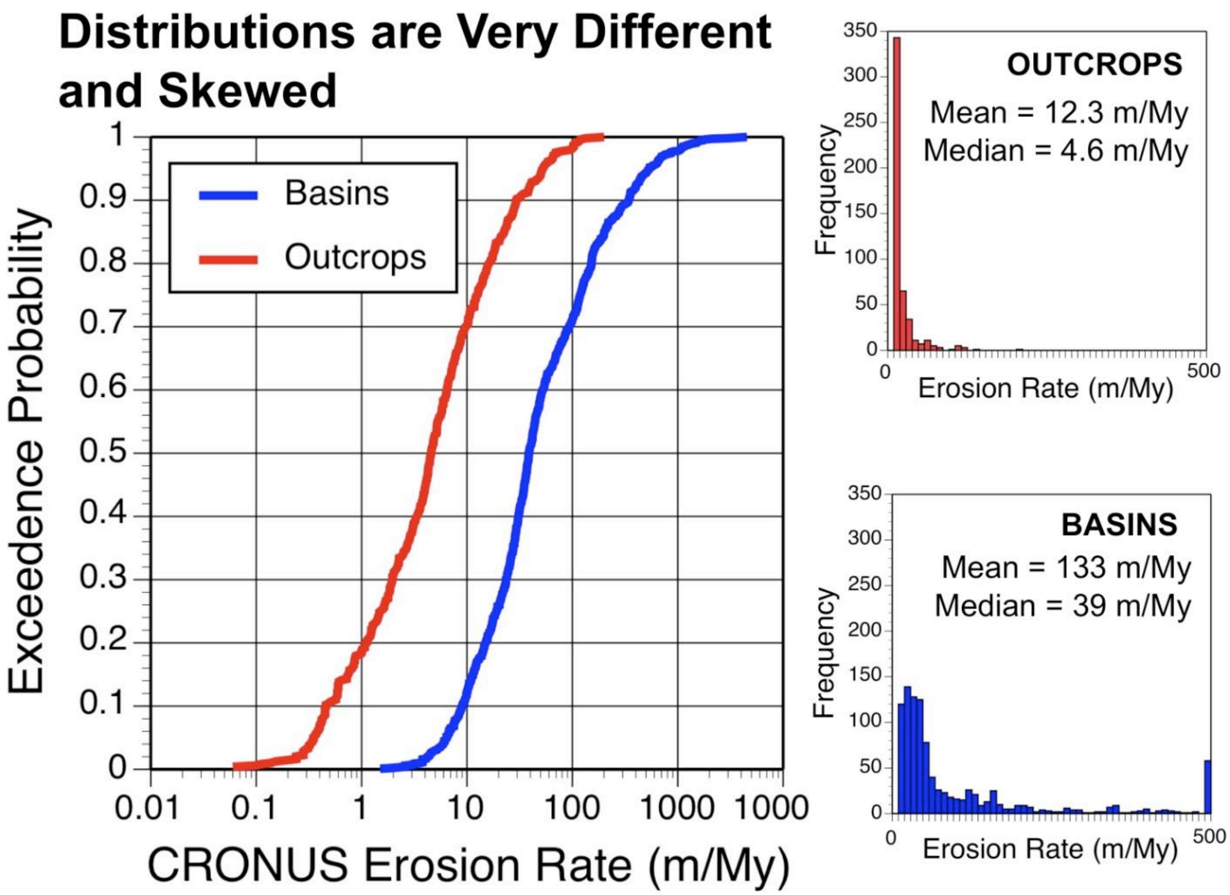

Figure 2. Distribution of bedrock outcrop and drainage-basin erosion rates. Cumulative probability plot illustrates the >10-fold difference between outcrop and basin erosion rates. NOTE. THIS IS A TEMPORARY FIGURE AND WILL BE UPDATED.

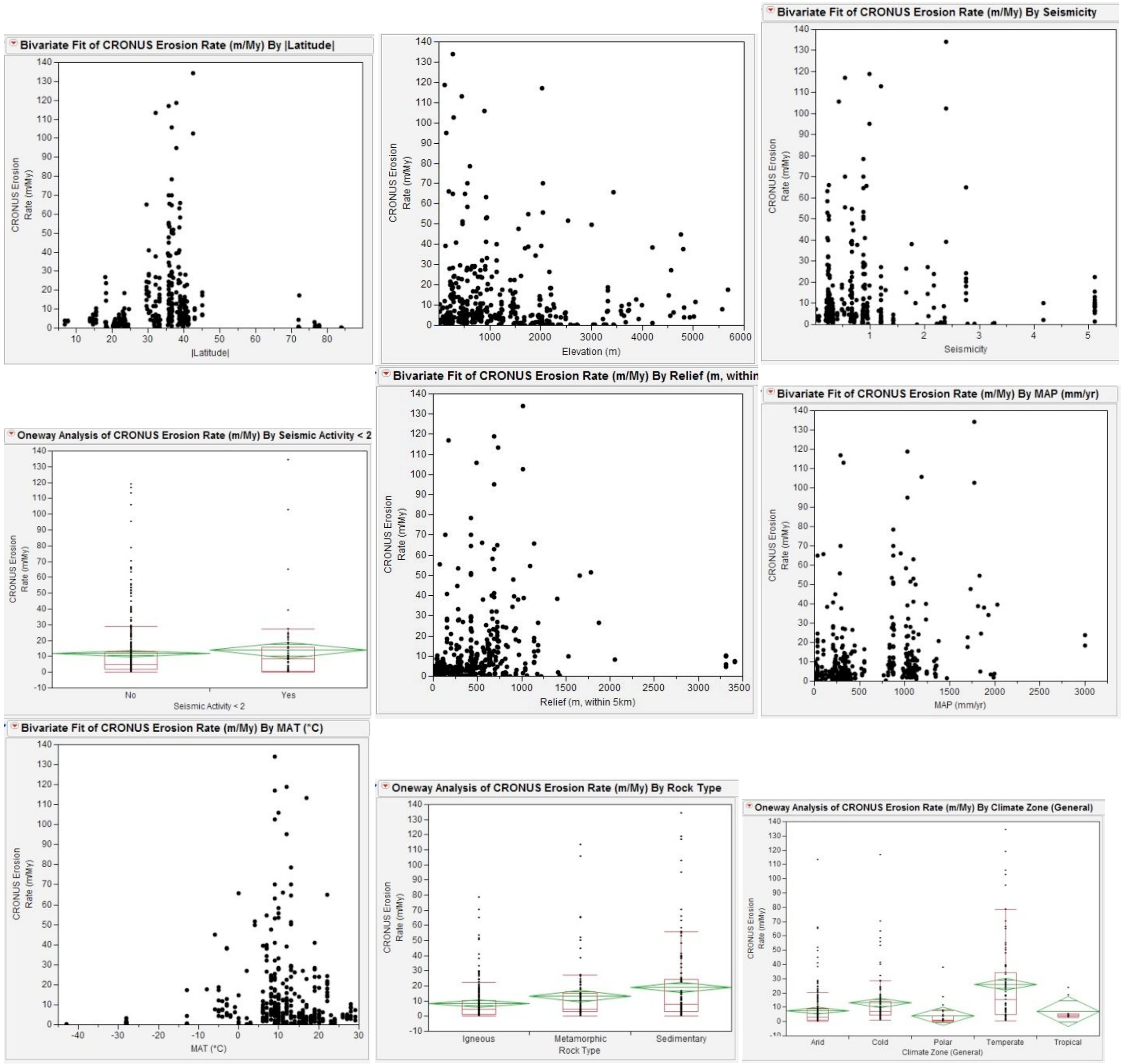

Figure 3. Bivariate analyses of outcrop erosion rate by numerical data and oneway analyses of outcrop erosion rate by nominal data categories. FIGURES ARE NOT IN FINAL-DRAFT FORM. PLEASE EXCUSE THE ROUGHNESS!

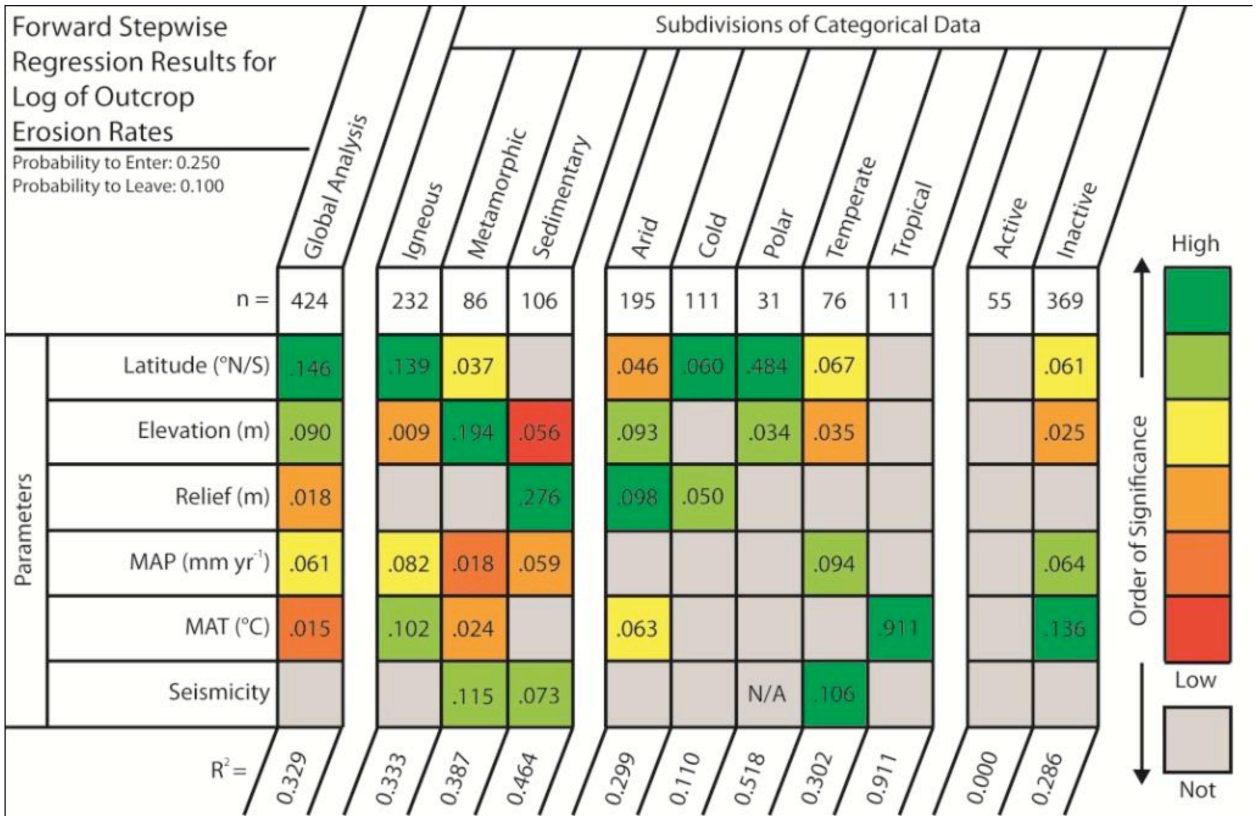

Figure 4a. Results of Forward stepwise regressions for bedrock outcrops. Colored tiles rank the significance of entered parameters. Numeric values in each grid cell represent the amount of improvement to the total R^2 value each parameter provides.

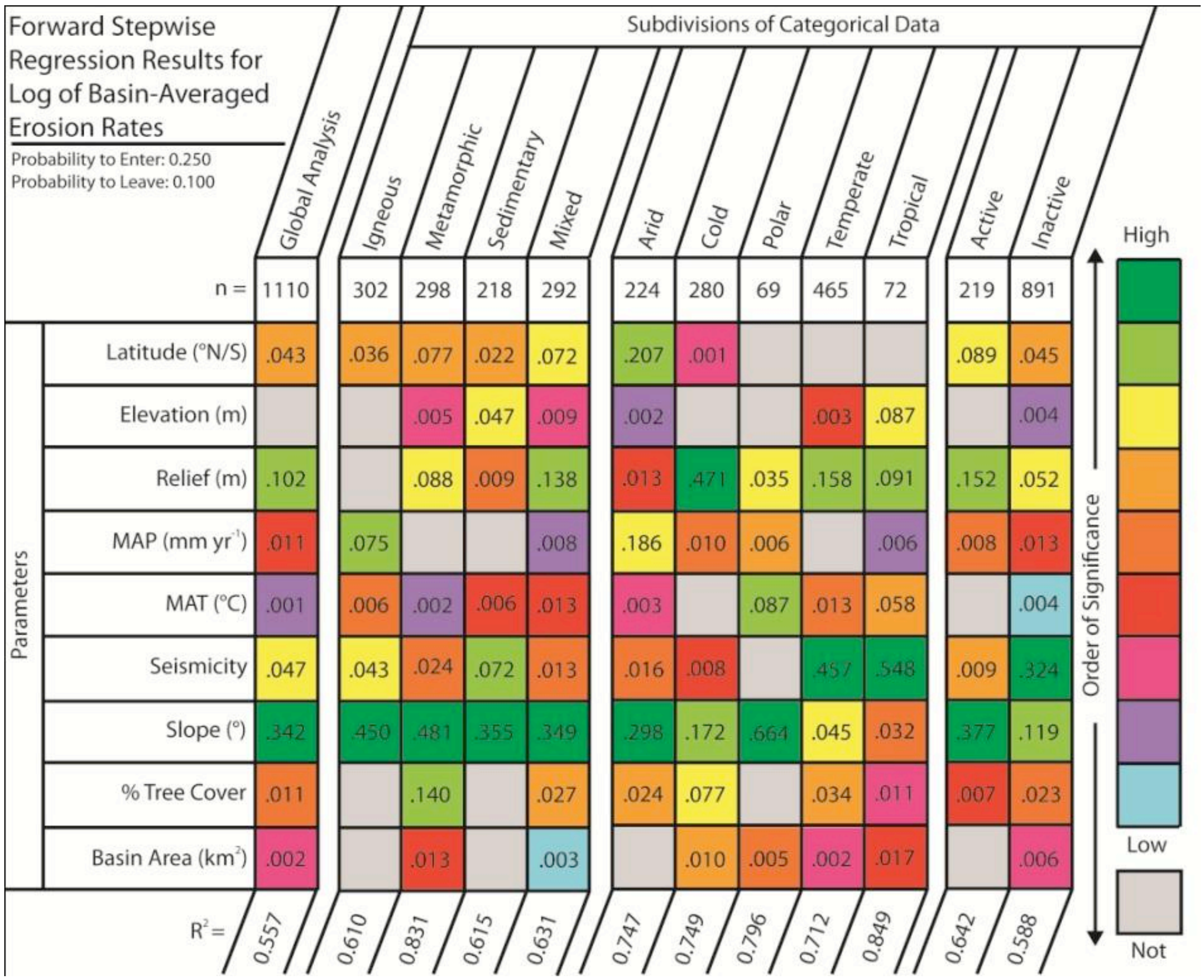

Figure 4b. Results of Forward stepwise regressions for drainage basins. Colored tiles rank the significance of entered parameters. Numeric values in each grid cell represent the amount of improvement to the total R^2 value each parameter provides.

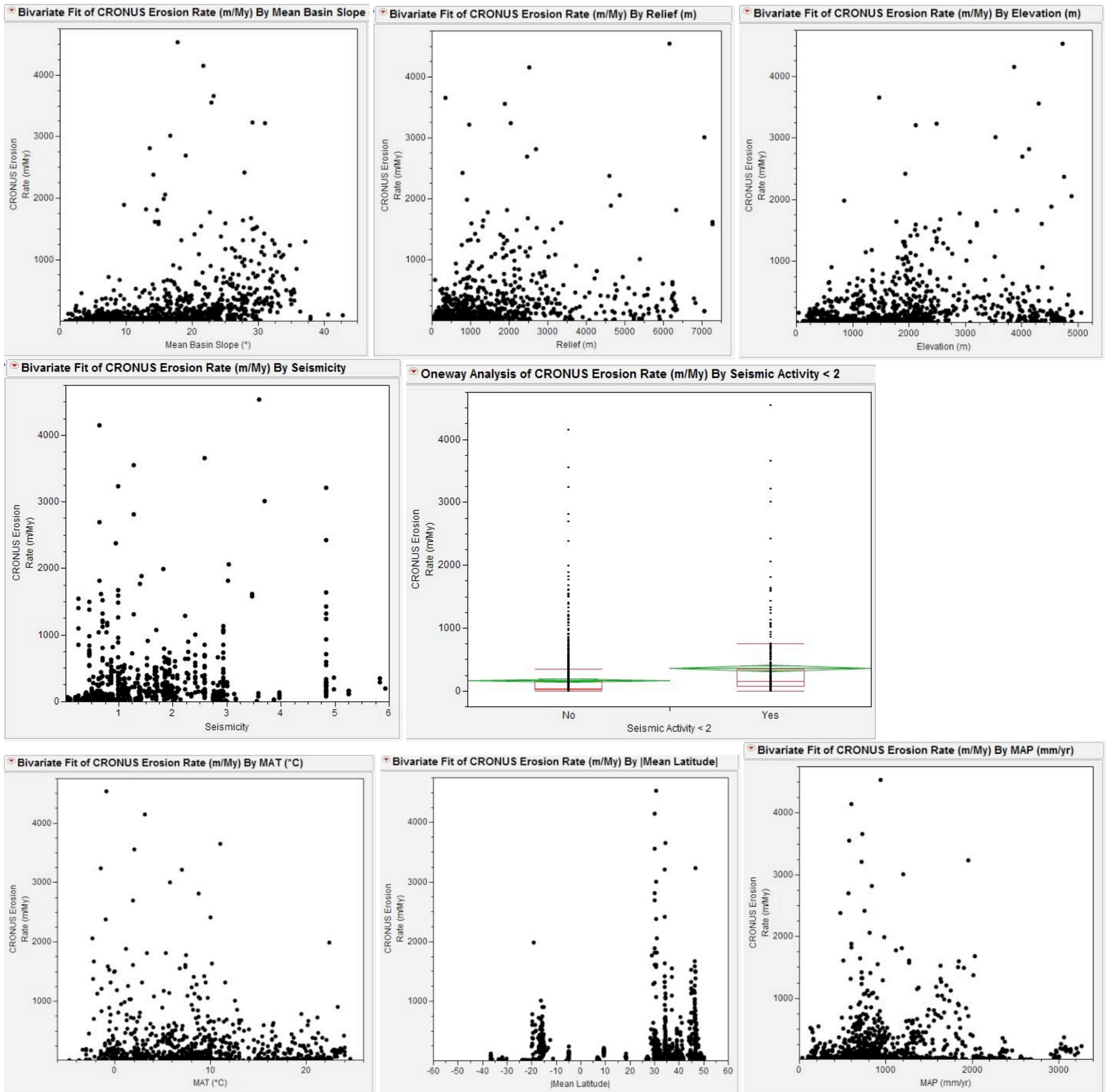
Bivariate Fit of CRONUS Erosion Rate (m/My) By Mean Basin Slope
CRONUS Erosion Rate (m/My)
Mean Basin Slope (°)
Bivariate Fit of CRONUS Erosion Rate (m/My) By Relief (m)
CRONUS Erosion Rate (m/My)
Relief (m)
Bivariate Fit of CRONUS Erosion Rate (m/My) By Elevation (m)
CRONUS Erosion Rate (m/My)
Elevation (m)
Bivariate Fit of CRONUS Erosion Rate (m/My) By Seismicity
CRONUS Erosion Rate (m/My)
Seismicity
Oneway Analysis of CRONUS Erosion Rate (m/My) By Seismic Activity < 2
CRONUS Erosion Rate (m/My)
No
Yes
Seismic Activity < 2
Bivariate Fit of CRONUS Erosion Rate (m/My) By MAT (°C)
CRONUS Erosion Rate (m/My)
MAT (°C)
Bivariate Fit of CRONUS Erosion Rate (m/My) By |Mean Latitude|
CRONUS Erosion Rate (m/My)
|Mean Latitude|
Bivariate Fit of CRONUS Erosion Rate (m/My) By MAP (mm/yr)
CRONUS Erosion Rate (m/My)
MAP (mm/yr)

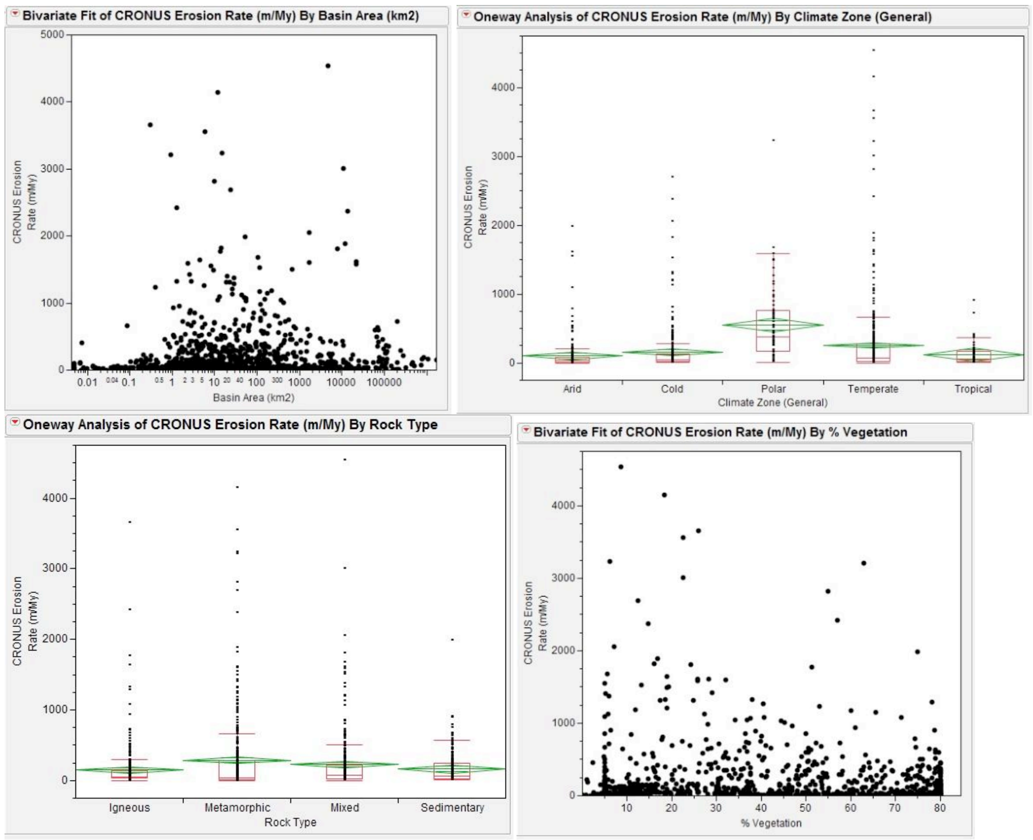

Figure 5. Bivariate analyses of drainage basin erosion rate by numerical data and oneway analyses of outcrop erosion rate by nominal data categories. FIGURES ARE NOT IN FINAL-DRAFT FORM. PLEASE EXCUSE THE ROUGHNESS!

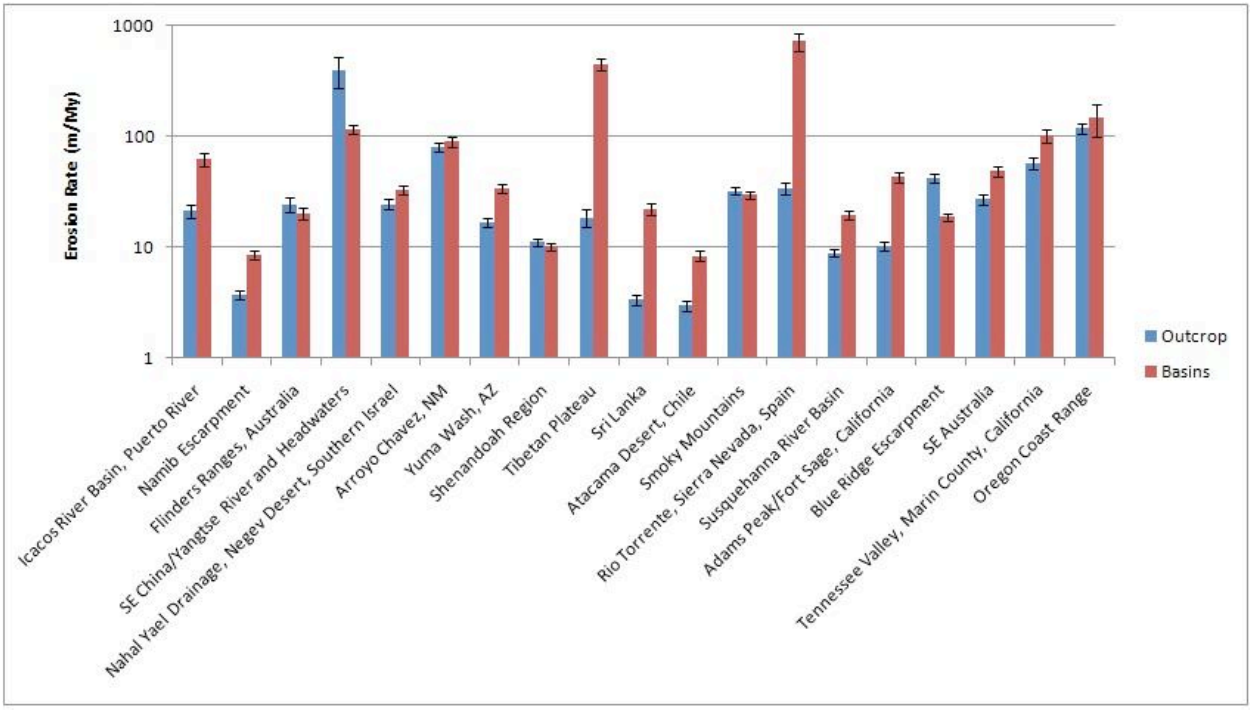

Figure 6. Bar plot comparing bedrock outcrop and drainage basin erosion rates at sites where both have been measured.

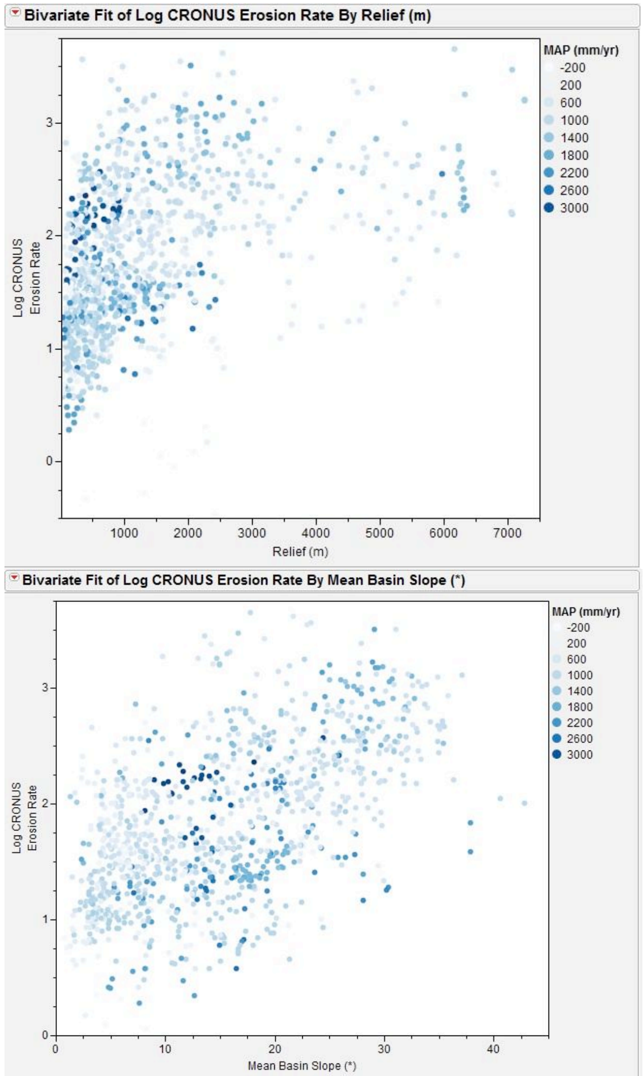

Figure 7. Drainage basin erosion rates plotted by relief (A) and slope (B) and symbolized by mean annual precipitation. No relationship is seen between higher amounts of relief or slope and mean annual precipitation.

References Cited

Abbühl, L. M., Norton, K. P., Schlunegger, F., Kracht, O., Aldahan, A., and Possnert, G., 2010, El Niño forcing on 10Be-based surface denudation rates in the northwestern Peruvian Andes?: Geomorphology, v. 123, p. 257-268.

Albrecht, A., Herzog, G. F., Klein, J., Dezfouly-Arjomandy, B., and Goff, F., 1993, Quaternary erosion and cosmic-ray-exposure history derived from 10Be and 26Al produced in situ; an example from Pajarito Plateau, Valles Caldera region: Geology, v. 21, no. 6, p. 551-554.

Balco, G., Stone, J. O., Lifton, N. A., and Dunai, T. J., 2008, A complete and easily accessible means of calculating surface exposure ages or erosion rates from 10Be and 26Al measurements: Quaternary Geochronology, v. 3, p. 174-195.

Belmont, P., Pazzaglia, F. J., and Gosse, J. C., 2007, Cosmogenic 10Be as a tracer for hillslope and channel sediment dynamics in the Clearwater River, western Washington State: Earth and Planetary Science Letters.

Belton, D. X., Brown, R. W., Kohn, B. P., Fink, D., and Farley, K. A., 2004, Quantitative resolution of the debate over antiquity of the central Australian landscape: implications for the tectonic and geomorphic stability of cratonic interiors: Earth and Planetary Science Letters, v. 219, no. 1-2, p. 21-34.

Bierman, P. R., Albrecht, A., Bothner, M., Brown, E., Bullen, T., Gray, L., and Turpin, L., 1998, Weathering, erosion and sedimentation, *in* Kendall, C., and McDonnell, J. J., eds., Isotope Tracers in Catchment Hydrology, Elsevier, p. 647-678.

Bierman, P. R., and Caffee, M., 2002, Cosmogenic exposure and erosion history of ancient Australian bedrock landforms: Geological Society of America Bulletin, v. 114, no. 7, p. 787-803.

Bierman, P. R., and Caffee, M. W., 2001, Slow rates of rock surface erosion and sediment production across the Namib Desert and escarpment, Southern Africa: American Journal of Science, v. 301, no. 4-5, p. 326-358.

Bierman, P. R., Clapp, E. M., Nichols, K. K., Gillespie, A. R., and Caffee, M., 2001, Using cosmogenic nuclide measurements in sediments to understand background rates of erosion and sediment transport,, *in* Harmon, R. S., and Doe, W. M., eds., Landscape Erosion and Evolution Modelling: New York, Kluwer, p. 89-116.

Bierman, P. R., Nichols, K. K., Matmon, A., Enzel, Y., Larsen, J., and Finkel, R., 2007, 10-Be shows that Namibian drainage basins are slowly, steadily and uniformly eroding: Quaternary International v. 167–168 no. 3, p. 33.

Bierman, P. R., Reusser, L. J., Nichols, K. K., Matmon, A., and Rood, D., 2009, Where is the sediment coming from and where is it going - A 10Be examination of the northern Queensland escarpment, Australia, 2009 Portland GSA Annual Meeting: Portland, Or.

Bierman, P. R., Reuter, J. M., Pavich, M., Gellis, A. C., Caffee, M. W., and Larsen, J., 2005, Using cosmogenic nuclides to contrast rates of erosion and sediment yield in a semi-arid, arroyo-dominated landscape, Rio Puerco Basin, New Mexico: Earth Surface Processes and Landforms, v. 30, no. 8, p. 935-953.

Bierman, P. R., and Steig, E., 1996, Estimating rates of denudation and sediment transport using cosmogenic isotope abundances in sediment: Earth Surface Processes and Landforms, v. 21, p. 125-139.

Binnie, S. A., Phillips, W. M., Summerfield, M. A., and Fifield, L. K., 2006, Sediment mixing and basin-wide cosmogenic nuclide analysis in rapidly eroding mountainous environments: Quaternary Geochronology v. 1, p. 4-14.

Binnie, S. A., Phillips, W. M., Summerfield, M. A., Fifield, L. K., and Spotila, J. A., 2008, Patterns of denudation through time in the San Bernardino Mountains, California: Implications for early-stage orogenesis Earth and Planetary Science Letters, v. In Press.

Brown, E. T., Bourles, D. L., Colin, F., Sanfo, Z., Raisbeck, G. M., and Yiou, F., 1994, The development of iron crust lateritic systems in Burkina Faso, West Africa examined with in-situ-produced cosmogenic nuclides: Earth and Planetary Science Letters, v. 124, p. 19-33.

Brown, E. T., Stallard, R. F., Larsen, M. C., Bourles, D. L., Raisbeck, G. M., and Yiou, F., 1998, Determination of predevelopment denudation rates of an agricultural watershed (Cayaguas River, Puerto Rico) using in-situ-produced ^{10}Be in river-borne quartz: Earth and Planetary Science Letters, v. 160, no. 3-4, p. 723-728.

Brown, E. T., Stallard, R. F., Larsen, M. C., Raisbeck, G. M., and Yiou, F., 1995, Denudation rates determined from the accumulation of in situ-produced ^{10}Be in the Luquillo Experimental Forest, Puerto Rico: Earth and Planetary Science Letters, v. 129, p. 193-202.

Chappell, J., Zheng, H., and Fifield, K., 2006, Yangtse River sediments and erosion rates from source to sink traced with cosmogenic 10Be: Sediments from major rivers: Palaeogeography, Palaeoclimatology, Palaeoecology, v. 241, no. 1, p. 79-94.

Clapp, E., Bierman, P. R., and Caffee, M., 2002, Using ^{10}Be and ^{26}Al to determine sediment generation rates and identify sediment source areas in an arid region drainage basin: Geomorphology, v. 45, no. 1,2, p. 89-104.

Clapp, E. M., Bierman, P. R., Nichols, K. K., Pavich, M., and Caffee, M., 2001, Rates of sediment supply to arroyos from upland erosion determined using in situ produced cosmogenic ^{10}Be and ^{26}Al: Quaternary Research (New York), v. 55, no. 2, p. 235-245.

Clapp, E. M., Bierman, P. R., Schick, A. P., Lekach, J., Enzel, Y., and Caffee, M., 2000, Sediment yield exceeds sediment production in arid region drainage basins: Geology, v. 28, no. 11, p. 995-998.

Cockburn, H. A. P., Brown, R. W., Summerfield, M. A., and Seidl, M. A., 2000, Quantifying passive margin denudation and landscape development using a combined fission-track thermochronology and cosmogenic isotope analysis approach: Earth and Planetary Science Letters, v. 179, no. 3-4, p. 429-435.

Cox, R., Bierman, P. R., Jungers, M., Rakotondrazafy, A. F. M., and Finkel, R. C., 2006, Just how fast does Madagascar erode? Evidence from ^{10}Be analysis of lavaka, slope, and river sediment: Geological Society of America *Abstracts with Programs*, v. 38, no. 7, p. 278.

Cyr, A. J., and granger, D. E., 2008, Dynamic equilibrium among erosion, river incision, and coastal uplift in the northern and central Apennines, Italy: Geology, v. 36, no. 2, p. 103-106.

Delunel, R., Beek, P. A. v. d., Carcaillet, J., Bourlès, D. L., and Valla, P. G., 2010, Frost-cracking control on catchment denudation rates: Insights from in situ produced 10Be concentrations in stream sediments (Ecrins–Pelvoux massif, French Western Alps): Earth and Planetary Science Letters, v. 293, p. 72-83.

DiBiase, R. A., Whipple, K. X., Heimsath, A. M., and Ouimet, W. B., 2010, Landscape form and millennial erosion rates in the San Gabriel Mountains, CA: Earth and Planetary Science Letters, v. 289, p. 134-144.

Dole, R. B., and Stabler, H., 1909, Denudation: USGS Water Supply Paper, v. 234, p. 78-93.

Duxbury, J., Bierman, P., Larsen, J., Pavich, M. J., Southworth, S., Miguéns-Rodríguez, M., and Freeman, S., accepted, Erosion rates in and around Shenandoah National Park, va, determined using analysis of cosmogenic ^{10}Be: American Journal of Science.

Elmore, D., and Phillips, F., 1987, Accelerator mass spectrometry for measurement of long-lived radioisotopes: Science, v. 236, p. 543-550.

Faure, G., and Nishiizumi, K., 1994, Exposure dating of quartz sandstone in the Transantarctic Mountains by cosmogenic (super 10) Be and 26Al, *in* Harte, B., ed., V. M. Goldschmidt Conference; extended abstracts Mineralogical Magazine 58A, no. A-K (199408), Mineralogical Society, London, United Kingdom, p. 268-269.

Ferrier, K. L., Kirchner, J. W., and Finkel, R. C., 2005, Erosion rates over millennial and decadal timescales at Caspar Creek and Redwood Creek, Northern California Coast Ranges: Earth Surface Processes and Landforms, v. 30, no. 8, p. 1025-1038.

Finnegan, N. J., Hallet, B., Montgomery, D. R., Zeitler, P., Stone, J., Anders, A. M., and Yuping, L., 2007, COUPLING OF ROCK UPLIFT AND RIVER INCISION IN THE NAMCHE BARWA-GYALA PERI MASSIF, TIBET: 2007 GSA Denver Annual Meeting.

Giardini, D., Grunthal, G., Shedlock, K. M., and Zhang, P., 1999, The GSHAP Global Seismic Hazard Map: Annali Di Geofisica, v. 42, no. 6, p. 1225-1230.

Granger, D. E., Kirchner, J. W., and Finkel, R., 1996, Spatially averaged long-term erosion rates measured from in situ-produced cosmogenic nuclides in alluvial sediments: Journal of Geology, v. 104, no. 3, p. 249-257.

Granger, D. E., Riebe, C. S., Kirchner, J. W., and Finkel, R. C., 2001, Modulation of erosion on steep granitic slopes by boulder armoring, as revealed by cosmogenic ^{26}Al and ^{10}Be: Earth and Planetary Science Letters, v. 186, no. 2, p. 269-281.

Guralnik, B., Matmon, A., Avni, Y., and Fink, D., 2010, 10Be exposure ages of ancient desert pavements reveal Quaternary evolution of the Dead Sea drainage basin and rift margin tilting: Earth and Planetary Science Letters, v. 290, p. 132-141.

Hack, J. T., 1975, Dynamic equilibrium and landscape evoluion, *in* Melhorn, W. N., and Flemal, R. C., eds., Theories of landform development: Binghamton, N.Y., SUNY Binghamton,, p. 87-102.

-, 1979, Rock control and tectonism, their importance in shaping the Appalachian highlands: U.S. Geological Survey professional paper, v. 1126-B, p. 17.

Hales, T. C., and Roering, J. J., 2007, Climatic controls on frost cracking and implications for the evolution of bedrock landscapes: Journal of Geophysical Research, v. 112.

Hancock, G., and Kirwan, M., 2007, Summit erosion rates deduced from 10Be: Implications for relief production in the central Appalachians: Geology, v. 35, no. 1, p. 89-92.

Heimsath, A., Chappel, J., Finkel, R. C., Fifield, K., and Alimanovic, A., 2006, Escarpment Erosion and Landscape Evolution in Southeastern Australia: SPECIAL PAPERS-GEOLOGICAL SOCIETY OF AMERICA, v. 398, p. 173.

Heimsath, A. M., Chappell, J., Dietrich, W. E., Nishiizumi, K., and Finkel, R. C., 2000, Soil production on a retreating escarpment in southeastern Australia: Geology, v. 28, no. 9, p. 787-790.

-, 2001a, Late Quaternary erosion in southeastern Australia: a field example using cosmogenic nuclides: Quaternary International, v. 83-85, p. 169-185.
Heimsath, A. M., Dietrich, W. E., Nishiizumi, K., and Finkel, R. C., 1997a, Cosmogenic nuclide and geomorphic determination of soil production in Northern California and coastal Oregon: Association of American Geographers 93rd annual meeting; abstracts Abstracts, Annual Meeting - Association of American Geographers, v. 1997, p. 110.
-, 1997b, The soil production function and landscape equilibrium: Nature (London), v. 388, no. 6640, p. 358-361.
-, 1999, Cosmogenic nuclides, topography, and the spatial variation of soil depth: Geomorphology, v. 27, no. 1-2, p. 151-172.
-, 2001b, Stochastic processes of soil production and transport; erosion rates, topographic variation and cosmogenic nuclides in the Oregon Coast Range: Earth Surface Processes and Landforms, v. 26, no. 5, p. 531-552.
Henck, A. C., Huntington, K. W., Stone, J. O., Montgomery, D. R., and Hallet, B., In Review, Spatial controls on erosion in the Three Rivers Region, southeastern Tibet and southwestern China: Earth and Planetary Science Letters.
Hewawasam, T., von Blackenburg, F., Schaller, M., and Kubik, P., 2003, Increase of human over natural erosion rates in tropical highlands constrained by cosmogenic nuclides: Geology, v. 31, no. 7, p. 597-600.
Hijmans, R. J., Cameron, S. E., Parra, J. L., Jones, P. G., and Jarvis, A., 2005, Very High Resolution Interpolates Climate Surfaces for Global Land Areas: International Journal of Climatology, v. 25, p. 1965-1978.
Hooke, R. L., 1994, On the efficacy of humans as geomorphic agents: GSA Today, v. 4, no. 9, p. 217,224-225.
-, 2000, On the history of humans as geomorphic agents: Geology, v. 28, no. 9, p. 843-846.
Insel, N., Ehlers, T. A., Schaller, M., Barnes, J. B., Tawackoli, S., and Poulsen, C. J., 2010, Spatial and temporal variability in denudation across the Bolivian Andes from multiple geochronometers: 2010, v. 122, p. 65-77.
Ivy-Ochs, S., Kober, F., Alfimov, V., Kubik, P. W., and Synal, H.-A., 2007, Cosmogenic 10Be, 21Ne and 36Cl in sanidine and quartz from Chilean ignimbrites: Nuclear Instruments and Methods in Physics Research B, v. 259, p. 588-594.
Jakica, S., Quigley, M. C., Sandiford, M., Clark, D., Fifield, K., and Alimanovic, A., 2010, Geomorphic and cosmogenic nuclide constraings on escarpment evolution in an intraplate setting, Darling Escarpment, Western Australia: Earth Surface Processes and Landforms.
Judson, S., 1968, Erosion of the land or what's happening to our continents: American Scientist, v. 56, p. 356-374.
Kirchner, J. W., Finkel, R. C., Riebe, C. S., Granger, D. E., Clayton, J. L., King, J. G., and Megahan, W. F., 2001, Mountain erosion over 10 yr, 10 k.y., and 10 m.y. time scales: Geology, v. 29, no. 7, p. 591-594.
Kober, F., Ivy-Ochs, S., Schlunegger, F., Baur, H., Kubik, P. W., and Wieler, R., 2007, Denudation rates and a topography-driven rainfall threshold in northern Chile: Multiple cosmogenic nuclide data and sediment yield budgets: Geomorphology, v. 83, p. 97-120.
Kober, F., Ivy-Ochs, S., Zeilinger, G., Schlunegger, F., Kubik, P. W., Baur, H., and Wieler, R., 2009, Complex multiple cosmogenic nuclide concentration and histories in the arid Rio

Lluta catchment, northern Chile: Earth Surface Processes and Landforms, v. 34, p. 398-412.
Lal, D., 1991, Cosmic ray labeling of erosion surfaces; in situ nuclide production rates and erosion models: Earth and Planetary Science Letters, v. 104, no. 2-4, p. 424-439.
Lal, D., Harris, N. B. W., Sharma, K. K., Gu, Z., Ding, L., Liu, T., Dong, W., Caffee, M. W., and Jull, A. J. T., 2003, Erosion history of the Tibetan Plateau since the last interglacial: constraints from the ¢rst studies of cosmogenic 10Be from Tibetan bedrock: Earth and Planetary Science Letters, v. 217, p. 33-42.
Matmon, A. S., Bierman, P., Larsen, J., Southworth, S., Pavich, M., Finkel, R., and Caffee, M., 2003, Erosion of an ancient mountain range, the Great Smoky Mountains, North Carolina and Tennessee: American Journal of Science, v. 303, p. 817-855.
Morel, P., von Blackenburg, F., Schaller, M., Kubik, P. W., and Hinderer, M., 2003, Lithology, landscape dissection and glaciation controls on catchment erosion as determined by cosmogenic nuclides in river sediment (the Wutach Gorge, Black Forest): Terra Nova, v. 15, no. 6, p. 398-404.
Nichols, K., Bierman, P., Finkel, R., and Larsen, J., 2005a, Long-Term (10 to 20 kyr) Sediment Generation Rates for the Upper Rio Chagres Basin Based on Cosmogenic ^{10}Be, *in* Harmon, R. S., ed., The Rio Chagres: A Multidisciplinary Profile of a Tropical Watershed, Kluwer Academic Publishers.
Nichols, K. K., Bierman, P., and Matmon, A., 2007, Deconvolving semi-arid landscape histories: insights from cosmogenic nuclides: Quaternary International, v. 167–168, no. 3, p. 305.
Nichols, K. K., Bierman, P. R., Caffee, M., Finkel, R., and Larsen, J., 2005b, Cosmogenically enabled sediment budgeting: Geology, v. 33, no. 2, p. 133-136.
Nichols, K. K., Bierman, P. R., Foniri, W. R., Gillespie, A. R., Caffee, M., and Finkel, R., 2006, Dates and rates of arid region geomorphic processes: GSA Today, v. 16, no. 8, p. 4-11.
Nichols, K. K., Bierman, P. R., Hooke, R. L., Clapp, E., and Caffee, M., 2002, Quantifying sediment transport on desert piedmonts using ^{10}Be and ^{26}Al: Geomorphology, v. 45, no. 1,2, p. 89-104.
Nishiizumi, K., Klein, J., Middleton, R., and Craig, H., 1990, Cosmogenic 10Be, 26Al, and 3He in olivine from Maui lavas: Earth and Planetary Science Letters, v. 98, no. 3-4, p. 263-265.
Nishiizumi, K., Lal, D., Klein, J., Middleton, R., and Arnold, J. R., 1986, Production of ^{10}Be and ^{26}Al by cosmic rays in terrestrial quartz in situ and implications for erosion rates: Nature, v. 319, no. 6049, p. 134-136.
Norton, K. P., Blanckenburg, F. v., and Kubik, P. W., 2010, Cosmogenic nuclide-derived rates of diffusive and episodic erosion in the glacially sculpted upper Rhone Valley, Swiss Alps: Earth Surface Processes and Landforms, v. 35, p. 651-662.
Norton, K. P., Blanckenburg, F. v., Schlunegger, F., Schwab, M., and Kubik, P. W., 2008, Cosmogenic nuclide-based investigation of spatial erosion and hillslope channel coupling in the transient foreland of the Swiss Alps: Geomorphology, v. 95, p. 474-486.
Ouimet, W. B., Whipple, K. X., and Granger, D. E., 2009, Beyond threshold hillslopes: Channel adjustment to base-level fall in tectonically active mountain ranges: Geology, v. 37, no. 7, p. 579-582.
Palumbo, L., Hetzel, R., Tao, M., and Li, X., 2009, Topographic and lithologic control on catchment-wide denudation rates derived from cosmogenic 10Be in two mountain ranges at the margin of NE Tibet: Geomorphology, v. 117, p. 130-142.

Peel, M. C., Finlayson, B. L., and McMahon, T. A., 2007, Updated world map of the K¨oppen-Geiger climate classification: Hydrology and Earth System Sciences, v. 11, p. 1633-1644.
Perg, L., Anderson, R., and Finkel, R., 2003, Use of cosmogenic radionuclides as a sediment tracer in the Santa Cruz littoral cell, California, USA: Geology, v. 31, p. 299-302.
Placzek, C. J., Matmon, A., Granger, D. E., Quade, J., and Niedermann, S., 2010, Evidence for active landscape evolution in the hyperarid Atacama from multiple terrestrial cosmogenic nuclides: Earth and Planetary Science Letters, v. 295, p. 12-20.
Portenga, E. W., Bierman, P. R., Trodick, C. D. J., and Rood, D. H., 2010, Low rates of bedrock outcrop erosion in the central Appalachian Mountains inferred from *In Situ* 10Be concentrations, *in* 2010 GSA Denver Annual Meeting, Denver, Colorado.
Quigley, M., Sandiford, M., Fifield, K., and Alimanovic, A., 2007a, Bedrock erosion and relief production in the northern Flinders Ranges, Australia: Earth Surface Processes and Landforms, v. 32, no. 6, p. 929.
Quigley, M., Sandiford, M., Fifield, L. K., and Alimanovic, A., 2007b, Landscape responses to intraplate tectonism: Quantitative constraints from 10Be nuclide abundances: Earth and Planetary Science Letters, v. 261, no. 1-2, p. 120-133.
Reinhardt, L. J., Bishop, P., Hoey, T. B., Dempster, T. J., and Sanderson, D. C. W., 2007, Quantification of the transient response to base-level fall in a small mountain catchment: Sierra Nevada, southern Spain Journal of Geophysical Research, v. 112, no. F03S05, p. 20.
Reuter, J., Bierman, P. R., Pavich, M., Gellis, A., Larsen, J., and Finkel, R., 2003, Long-term sediment generation rates derived from 10Be in river sediment of the Susquehanna River Basin, in "channeling through time: Landscape evolution, land use change, and stream restoration in the lower Susquehanna Basin", *in* Merritts, D., Walter, R., and de Wet, A., eds., Southeastern Friends of the Pleistocene Fall 2003 Guidebook, p. 48-55.
Reuter, J. M., Bierman, P. R., Pavich, M., Larsen, J., and Finkel, R., 2006, ^{10}Be estimates of erosion rates in the Susquehanna River basin: Implications for models of Appalachian geomorphology and consideration of rates in a global context: Geological Society of America *Abstracts with Programs*, v. 38, no. 7, p. 278.
Riebe, C. S., Kirchner, J. W., and Finkel, R. C., 2003, Long-term rates of chemical weathering and physical erosion from cosmogenic nuclides and geochemical mass balance: Geochimica et Cosmochimica Acta, v. 67, no. 22, p. 4411-4427.
Riebe, C. S., Kirchner, J. W., Granger, D. E., and Finkel, R. C., 2000, Erosional equilibrium and disequilibrium in the Sierra Nevada, inferred from cosmogenic ^{26}Al and ^{10}Be in alluvial sediment: Geology, v. 28, no. 9, p. 803-806.
-, 2001, Strong tectonic and weak climatic control of long-term chemical weathering rates: Geology, v. 29, no. 6, p. 511–514.
Safran, E. B., Bierman, P. R., Aalto, R., Dunne, T., Whipple, K. X., and Caffee, M., 2005, Erosion rates driven by channel network incision in the Bolivian Andes: Earth Surface Processes and Landforms, v. 30, no. 8, p. 1007-1024.
Saunders, I., and Young, A., 1983, Rates of surface processes on slopes, slope retreat, and denudation: Earth Surface Processes and Landforms, v. 8, p. 473-501.
Schaller, M., von Blanckenburg, F., Hovius, N., and Kubik, P. W., 2001, Large-scale erosion rates from In situ-produced cosmogenic nuclides in European river sediments: Earth and Planetary Science Letters, v. v. 188, p. 441-458.

Small, E. E., Anderson, R. S., Repka, J. L., and Finkel, R., 1997, Erosion rates of alpine bedrock summit surfaces deduced from in situ ^{10}Be and ^{26}Al: Earth and Planetary Science Letters, v. 150, no. 3-4, p. 413-425.

Stock, G. M., Frankel, K. L., Ehlers, T. A., Schaller, M., Briggs, S. M., and Finkel, R. C., 2009, Spatial and temporal variations in denudation of the Wasatch Mountains, Utah, USA: Lithosphere, v. 1, no. 1, p. 34-40.

Sullivan, C. L., Bierman, P. R., Reusser, L., Larsen, J., Pavich, M. J., and Finkel, R. C., accepted, Erosion and landscape evolution of the Blue Ridge escarpment, southern Appalachian Mountains: Earth Surface Processes and Landforms.

Summerfield, M. A., and Hulton, N. J., 1994, Natural controls of fluvial denudation rates in major world drainage basins: Journal of Geophysical Research, v. 99, no. B7, p. 13871-13883.

Syvitski, J. P. M., and Milliman, J. D., 2007, Geology, Geography, and Humans Battle for Dominance over the Delivery of Fluvial Sediment to the Coastal Ocean: The Journal of Geology, v. 115, p. 1-19.

Syvitski, J. P. M., Vorosmarty, C. J., Kettner, A. J., and Green, P., 2005, Impact of Humans on the Flux of Terrestrial Sediment to the Global Coastal Ocean: Science, v. 308, p. 376-380.

Tomkins, K. M., Humphreys, G. S., Wilkinson, M. T., Fink, D., Hesse, P. P., Doerr, S. H., Shakesby, R. A., Wallbrink, P. J., and Blake, W. H., 2007, Contemporary versus long-term denudation along a passive plate margin: the role of extreme events: Earth Surface Processes and Landforms, v. 32, no. 7, p. 1013.

Trimble, S. W., 1977, The fallacy of stream equilibrium in contemporary denudation studies: American Journal of Science, v. 277, p. 876-887.

Vanacker, V., von Blanckenburg, F., Hewawasam, T., and Kubik, P. W., 2007, Constraining landscape development of the Sri Lankan escarpment with cosmogenic nuclides in river sediment: Earth and Planetary Science Letters, v. 253, no. 3-4, p. 402-414.

Vance, D., Bickle, M., Ivy-Ochs, S., and Kubik, P. W., 2003, Erosion and exhumation in the Himalaya from cosmogenic isotope inventories of river sediments: Earth and Planetary Science Letters, v. 206, p. 273-288.

von Blanckenburg, F., Hewawasam, T., and Kubik, P. W., 2004, Cosmogenic nuclide evidence for low weathering and denudation in the wet, tropical highlands of Sri Lanka: Journal of Geophysical Research, v. 109, no. F3.

Ward, I. A. K., Nanson, G. C., Head, L. M., Fullagar, R. L. K., Price, D. M., and Fink, D., 2005, Late Quaternary landscape evolution in the Keep River region, northwestern Australia: Quaternary Science Reviews, v. 24, no. 16-17, p. 1906-1922.

Weissel, J. K., and Seidl, M. A., 1998, Inland propagation of erosional escarpments and river profile evolution across the southeast Australian passive continental margin: Geophysical Monograph, v. 107, p. 189-206.

Wilkinson, B. H., and McElroy, B. J., 2007, The impact of humans on continental erosion and sedimentation: Geological Society of America Bulletin, v. 119, no. 1, p. 140-156.

Wittmann, H., Blanckenburg, F. v., Guyot, J. L., Maurice, L., and Kubik, P. W., 2009, From source to sink: Preserving the cosmogenic 10Be-derived denudation rate signal of the Bolivian Andes in sediment of the Beni and Mamoré foreland basins: Earth and Planetary Science Letters, v. 288, p. 463-474.

Wittmann, H., Blanckenburg, F. v., Kruesmann, T., Norton, K. P., and Kubik, P. W., 2007, Relation between rock uplift and denudation from cosmogenic nuclides in river sediment in the Central Alps of Switzerland: Journal of Geophysical Research, v. 112, no. F04010.

Zeitler, P. K., Meltzer, A. S., Koons, P. O., Craw, D., Hallet, B., Chamberlain, C. P., Kidd, W. S. F., Park, S. K., Seeber, L., Bishop, M., and Shroder, J., 2001, Erosion, Himalayan geodynamics, and the geomorphology of metamorphism: GSA Today, v. 11, no. 1, p. 4-9.